

# *Northern Hemisphere monsoon response to mid-Holocene orbital forcing and greenhouse gas-induced global warming*

Article

Accepted Version

D'Agostino, R., Bader, J., Bordoni, S., Ferreira, D. ORCID: <https://orcid.org/0000-0003-3243-9774> and Jungclaus, J. (2019) Northern Hemisphere monsoon response to mid-Holocene orbital forcing and greenhouse gas-induced global warming. *Geophysical Research Letters*, 46 (3). pp. 1591-1601. ISSN 0094-8276 doi: 10.1029/2018GL081589 Available at <https://centaur.reading.ac.uk/81488/>

It is advisable to refer to the publisher's version if you intend to cite from the work. See [Guidance on citing](#).

To link to this article DOI: <http://dx.doi.org/10.1029/2018GL081589>

Publisher: American Geophysical Union

All outputs in CentAUR are protected by Intellectual Property Rights law, including copyright law. Copyright and IPR is retained by the creators or other copyright holders. Terms and conditions for use of this material are defined in the [End User Agreement](#).

[www.reading.ac.uk/centaur](http://www.reading.ac.uk/centaur)

**CentAUR**

Central Archive at the University of Reading

Reading's research outputs online

# Northern Hemisphere monsoon response to mid-Holocene orbital forcing and greenhouse gas-induced global warming

Roberta D’Agostino<sup>1</sup>

Jürgen Bader<sup>1,2</sup>

Simona Bordoni<sup>3</sup>

David Ferreira<sup>4</sup>

Johann Jungclauss<sup>1</sup>

<sup>1</sup>Max Planck Institute for Meteorology, Hamburg, Germany.

<sup>2</sup>Uni Climate, Uni Research and the Bjerknes Centre for Climate Research, Bergen, Norway.

<sup>3</sup>California Institute of Technology, Pasadena, California.

<sup>4</sup>Department of Meteorology, University of Reading, United Kingdom

## Key Points:

- Different mechanisms mediate the response of Northern Hemisphere monsoons under future global warming and mid-Holocene forcing.
- Northern Hemisphere monsoons intensify more strongly in mid-Holocene than in future climate despite a larger warming in the latter.
- As an emergent constraint for future projections, tropical circulation weakening limits monsoon rainfall increase with global warming.

---

Corresponding author: Roberta D’Agostino, Max Planck Institute for Meteorology, Bundesstr. 53, 20146, Hamburg, Germany, [roberta.dagostino@mpimet.mpg.de](mailto:roberta.dagostino@mpimet.mpg.de)

## Abstract

Precipitation and circulation patterns of Northern Hemisphere monsoons are investigated in Coupled Model Intercomparison Project phase 5 simulations for mid-Holocene and future climate scenario rcp8.5. Although both climates exhibit Northern Hemisphere warming and enhanced inter-hemispheric thermal contrast in boreal summer, changes in the spatial extent and rainfall intensity in future climate are smaller than in mid-Holocene for all Northern Hemisphere monsoons except the Indian monsoon. A decomposition of the moisture budget in thermodynamic and dynamic contributions suggests that under future global warming the weaker response of the African, Indian and North American monsoons results from a compensation between both components. The dynamic component, primarily constrained by changes in net energy input over land, determines instead most of the mid-Holocene land monsoonal rainfall response.

## 1 Introduction

The mid-Holocene was a period around 6,000 years ago, when insolation changes driven by Earth's axis precession changes resulted in a general warming of the Northern Hemisphere (NH), an enhanced insolation seasonality and a stronger inter-hemispheric thermal contrast compared with present-day boreal summer (Zhao & Harrison, 2012). In agreement with expectations based on recent theories of monsoons (Schneider et al., 2014), these insolation-driven temperature changes resulted in a robust increase in monsoonal rainfall during the last interglacial and the mid-Holocene in North Africa (Weldeab et al., 2007; Tjallingii et al., 2008), India (Schulz et al., 1998; Fleitmann et al., 2003), East Asia (Liu & Ding, 1998; Yuan et al., 2004; Wang et al., 2008; Lézine et al., 2011; Hély & Lézine, 2014; Tierney & Pausata, 2017) and northernmost South America (Haug et al., 2001) as shown by proxy reconstructions. This wettening tendency is also observed in a number of climate simulations from the Paleoclimate Model Intercomparison Project (PMIP) (Zhao et al., 2005; Zhao & Harrison, 2012) under mid-Holocene forcing, despite difficulties in reproducing the magnitude and northward expansion of rainfall as suggested by proxy data, particularly over the Sahara (Braconnot et al., 1999; Liu et al., 2007; Braconnot et al., 2012; Harrison et al., 2015; Boos & Korty, 2016). Some recent studies show better agreement with proxies on mid-Holocene precipitation in models that account for interactive vegetation or realistic vegetation cover over the Sahara (Vamborg et al., 2010; Swann et al., 2014; Pausata et al., 2016; Egerer et al., 2018; Lu et al., 2018), but sim-

ulations with precipitation and vegetation changes consistent with proxies have yet to be achieved.

Similar to mid-Holocene, the Representative Concentration Pathway global warming scenario rcp8.5 projects a warming of the Northern relative to the Southern Hemisphere and an enhanced inter-hemispheric thermal contrast resulting from stronger warming over land than over ocean (Sutton et al., 2007; Compo & Sardeshmukh, 2009; Jones et al., 2013; Acosta Navarro et al., 2017). These elements all support a tendency toward increased global monsoon rainfall strength and extent (Trenberth et al., 2000; Hsu et al., 2012, 2013; Kitoh et al., 2013; Lee & Wang, 2014) associated with reinforced low-level moisture convergence (Hsu et al., 2012; Kitoh et al., 2013; Lee & Wang, 2014). On a regional scale, evaluation of Coupled Model Intercomparison Project phase 3 and 5 (CMIP3 and CMIP5) simulations has indicated a wettening of the Asian monsoon (Kitoh et al., 2013; Endo & Kitoh, 2014) but has shown poor agreement in the African monsoon region because of competing effects of CO<sub>2</sub> increase and SST biases on the modelled West African monsoon response (Biasutti, 2013; Gaetani et al., 2017). Projections of the North American monsoon remain more inconclusive, with most models projecting a delay in the monsoon season with no robust changes in its summer mean intensity (Cook & Seager, 2013; Seth et al., 2013, 2011). The extent to which this might be a result of existing biases in the simulations of the present-day monsoon climatology remains a topic of debate (Pascale et al., 2017).

Despite a different global mean temperature response, the mean warming and the enhanced inter-hemispheric temperature contrast would suggest a strengthening and widening of NH monsoons in both climates relative to pre-industrial conditions (Tab. S2). Nevertheless, how similar the resulting regional monsoon responses are, remains unknown.

The energetic view of monsoons as moist energetically direct circulations tightly connected to the global Hadley cell (Bordoni & Schneider, 2008; Schneider et al., 2014; Biasutti et al., 2018) rather than as sea-breeze circulations driven by land-ocean temperature contrast (Webster & Fasullo, 2002; Fasullo & Webster, 2003; Fasullo, 2012; Gadgil, 2018) might provide some insight into the differing response of NH monsoons to mid-Holocene and rcp8.5 scenario. In this view, monsoons are fundamental components of the tropical overturning circulation, and, like the global mean Hadley cell, they export moist static energy (MSE) away from their ascending branches and precipitation max-

ima. If eddy energy fluxes are negligible, this implies that net energy input (NEI) into the atmospheric column given by the difference between top-of-atmosphere radiative and surface energy fluxes is primarily balanced by divergence of vertically integrated mean MSE flux (Chou et al., 2001; Merlis et al., 2013; Boos & Korty, 2016, see Eq. (3) below). Not surprisingly, the MSE budget has therefore provided the theoretical framework to understand the response of monsoons to different surface heat capacity (i.e. ocean versus land) (Chou et al., 2001), changes in atmospheric dynamics (Tanaka et al., 2005; Vecchi & Soden, 2007), in tropical tropospheric stability (Neelin et al., 2003), and in vegetation (Kutzbach et al., 1996; Claussen & Gayler, 1997; Broström et al., 1998; Claussen et al., 2013).

Changes in inter-hemispheric contrast in NEI, such as for instance those driven by precession-induced insolation changes, require anomalous meridional energy transport to restore energy balance. To the extent that during the summer most of this transport is accomplished by monsoonal circulations (Heaviside & Czaja, 2013; Walker, 2017), this would imply a shift of the monsoonal circulation ascending branches and precipitation maxima into the hemisphere with increased NEI and, possibly, an associated circulation strengthening (Schneider et al., 2014; Bischoff et al., 2017). It is important to note, however, that the MSE budget constrains the energy transport rather than the circulation strength itself (Merlis et al., 2013; Hill et al., 2015). The degree to which changes in energy transport implied by a given radiative forcing are accomplished through just changes in circulation strength or also changes in energy stratification (or gross moist stability, Neelin and Held, 1987) is not fully understood.

Here, we investigate the NH monsoon response in CMIP5 simulations under rcp8.5 and mid-Holocene forcing factors. Given the stronger thermal contrast between hemispheres and land versus ocean in rcp8.5 than in mid-Holocene one might expect that monsoon rainfall and extent would be greater in the former than in the latter. However, we will show that the opposite is true. Mechanisms of this differing monsoon response are investigated by decomposing the anomalous moisture budget in thermodynamic and dynamic components. The dynamic component is further related to NEI changes, to better understand why monsoons respond differently to different climate forcings and to explore to what extent the mid-Holocene may be considered as an analogue of future greenhouse gas-induced warming.

## 2 Data and Methods

We leverage mid-Holocene, piControl and rcp8.5 experiments that are available in CMIP5 archives. We use the first ensemble member (r1i1p1) of nine available models with all three experiments (i.e., bcc-csm-1-1, CCSM4, CNRM-CM5, CSIRO-Mk3-6-0, FGOALS-g2, HadGEM2-ES, IPSL-CM5A-LR, MIROC-ESM and MRI-CGCM3, see Table SI1). All datasets are interpolated to a common  $1^\circ \times 1.25^\circ$  latitude/longitude grid and to 17 pressure levels.

June to September (JJAS) climatologies are calculated for the last 30 years of rcp8.5, for the period 1850 - 2005 of piControl and for the last 100 years of mid-Holocene simulations. September is also included in the summer season, to account for seasonality delays in the Hadley and monsoonal circulations in both mid-Holocene and rcp8.5 (Seth et al., 2010; Dwyer et al., 2012; Seth et al., 2013; D’Agostino et al., 2017).

Changes in monsoon extent and strength are assessed using the following metrics: the monsoon extent is the land-only area where annual precipitation range, defined as the difference between summer and winter rainfall, exceeds 2 mm/day for each monsoon domain. The selected threshold warrants a concentrated summer rainy season and distinguishes monsoons from year-round rainy regimes (Zhou et al., 2008; Liu et al., 2009; Hsu et al., 2012). Choosing different definitions to calculate land-monsoon area (e.g. local summer precipitation exceeding 35%, 40%, 50% of the annual rainfall) does not significantly affect our results. The monsoon strength is the average summer rainfall calculated in each monsoon domain, specifically (see boxes in Fig. 1):

1. African monsoon ( $5^\circ$  to  $23.3^\circ$  N,  $20^\circ$  W to  $40^\circ$  E).
2. Indian monsoon ( $5^\circ$  to  $23.3^\circ$  N,  $70^\circ$  to  $120^\circ$  E).
3. North American monsoon ( $5^\circ$  to  $30^\circ$  N,  $120^\circ$  W to  $40^\circ$  W).

We also consider the whole NH tropical land-monsoon area (NHM,  $5^\circ$  to  $30^\circ$  N,  $0$  to  $360^\circ$  E). We exclude from our analyses the East Asian monsoon because its dynamics is related to shifts of the Pacific Subtropical High and interactions between the jet-stream and the Asian topography rather than to ITCZ seasonal migration and regional Hadley cell dynamics (Chen & Bordoni, 2014; Zhisheng et al., 2015). Following Trenberth and Guillemot (1995), the linearized anomalous moisture budget is decomposed into thermodynamic, dynamic components and a residual (*Res*) as:

$$\rho_w g \delta(P - E) = - \int_0^{p_s} \nabla \cdot (\delta \bar{q} \bar{\mathbf{u}}_{\text{piControl}}) dp - \int_0^{p_s} \nabla \cdot (\bar{q}_{\text{piControl}} \delta \bar{\mathbf{u}}) dp - Res, \quad (1)$$

where overbars indicate monthly means,  $(P-E)$  is precipitation minus evaporation,  $p$  is pressure,  $q$  is specific humidity,  $\bar{\mathbf{u}}$  is the horizontal vector wind, and  $\rho_w$  is the water density.  $\delta$  indicates the difference between each experiment (mid-Holocene or rcp8.5) and the reference climate (piControl) as:

$$\delta(\cdot) = (\cdot)_{\text{mid-Holocene or rcp8.5}} - (\cdot)_{\text{piControl}}. \quad (2)$$

In Eq. (1), the first term on the right-hand side is the thermodynamic contribution (TH): it represents changes in moisture flux convergence arising from changes in moisture, which generally follow the Clausius-Clapeyron relation for negligible relative humidity changes (e.g. Held and Soden, 2006). The second term in Eq. (1), the dynamic contribution (DY), involves changes in winds with unchanged moisture, and is mostly related to changes in the mean atmospheric flow. The third term describes the residual ( $Res$ ) which accounts for transient eddy contribution and surface quantities as described in the Supplementary Information.

Changes in the DY contribution to monsoonal precipitation changes are related to patterns of anomalous NEI, as any anomalous NEI in monsoonal regions will require changes in MSE export by the mean circulation in steady state:

$$\nabla \cdot \{\bar{\mathbf{u}}\bar{h}\} = NEI = R_{TOA} - F_{sfc}, \quad (3)$$

where  $\{\bar{\mathbf{u}}\bar{h}\}$  is the vertically integrated MSE flux,  $R_{TOA}$  the net top-of-atmosphere radiative fluxes and  $F_{sfc}$  the sum of the surface radiative and turbulent enthalpy fluxes.

### 3 Results

The future rcp8.5 and the past mid-Holocene climates are associated, respectively, with a strong (+4.2 K) and a weak (+0.3 K) global warming signal relative to piControl (Fig. 1, upper panels; Table S2). They also exhibit higher inter-hemispheric thermal contrasts (+10.0 K and +9.7 K compared to +9.2 K for piControl, see Table S2). However, the precipitation difference between rcp8.5 and mid-Holocene (Fig. 1, lower panel)



reveals a complex pattern of relative drying and wettening, reflective of a general tendency towards land drying and ocean wettening in rcp8.5, and land wettening and ocean drying in mid-Holocene.

To explain these differences in the precipitation response, we analyze the anomalous moisture budget of the two climates relative to piControl. This analysis shows how changes in net precipitation  $\delta(P-E)$  (see Eq. (1)) are primarily due to changes in precipitation alone, with changes in evaporation being negligible both in the multi-model mean (Figure S1 and S2) and in each individual model (not shown). Relative to piControl, precipitation in the African and Indian monsoons generally increases in mid-Holocene, while it decreases in the North American monsoon and increases in the Indian monsoon in rcp8.5. Figure 2 shows a general wettening of African and Indian monsoons in mid-Holocene relative to piControl, while in rcp8.5 the North American monsoon dries and the Indian monsoon wettens. The drying in the North American monsoon seen under rcp8.5 in the models considered in this study is at odds with previously published studies, which suggest no robust changes in the mean monsoon precipitation, but is in agreement with simulations in which SST biases in the North Atlantic are corrected with flux adjustment (Pascale et al., 2017). These ensemble mean  $(P-E)$  changes are robust as they occur in at least 8 out of 9 models considered here (stippled areas in Fig. 2), but models disagree on the magnitude of these changes. However, while in mid-Holocene models robustly produce wettening in the African equatorial rain belt and the sub-Saharan region, particularly in those models with active land module (i.e. bcc-csm1-1, CCSM4, CNRM-CM5, IPSL-CM5A-LR, FGOALS-g2, Had-GEM-ES, MIROC-ESM), there is less consensus on net precipitation changes in rcp8.5. Only CCSM4 shows a wettening of equatorial Africa; other models show decreased or no change in monsoonal precipitation (not shown).

It is noteworthy that, on a global scale (including changes over land as well as over oceans), rcp8.5 exhibits a robust shift of tropical precipitation towards the near-equatorial ocean relative to piControl (Fig. 2c). This tendency is also consistent with the projected squeezing of rain belts around the equator and the narrowing of the ITCZ in rcp8.5 (Byrne & Schneider, 2016). These findings however highlight that global ITCZ changes are not a good indicator of the land monsoon changes.

It is readily apparent from Figs. 1 and 2 that the mid-Holocene monsoon response is not a weaker version of the rcp8.5 response. Even more surprisingly, the simulated land monsoon changes are almost systematically smaller in rcp8.5 than in mid-Holocene, despite stronger global mean temperature increase and a slightly larger inter-hemispheric thermal contrast in the former than in the latter. In fact, both extent and strength of individual monsoons and the global NH land monsoon are projected to increase more in mid-Holocene than in rcp8.5. The notable exception to this general pattern is the Indian monsoon, whose strength increases more in rcp8.5 (Tab. 1).

To explain why the monsoon response is weaker under future global warming relative to the mid-Holocene, we decompose  $\delta(P-E)$  in TH and DY contributions as described in Section 2. Each of these components is shown in Figure S3 and S4; Results are summarized in Fig. 3 by averaging these components in each monsoon domain, where annual-range precipitation exceed 2 mm/day. The magnitude of the residual relative to the other components is also shown.

Fig. 3 reveals a striking contrast in the response in the two climates: in mid-Holocene, the DY term dominates the anomalous moisture budget in the African and Indian monsoon regions and in the overall NH monsoon domain. Only in the North American monsoon region does this term contribute marginally to the anomalous moisture budget (Fig. 3, and Fig. S3b). The DY component increases NH land precipitation through increased moisture convergence there (Fig. S3; see methods in Supplementary Information). Likewise, drying over near-equatorial oceans is associated with weaker wind convergence, especially in the Atlantic sector. Therefore, the enhanced African and Indian monsoonal rainfall in mid-Holocene is due to a strengthening of the mean flow. On the other hand, the TH component plays a secondary role in the mid-Holocene net precipitation increase in all monsoon domains, except in the North American monsoon (Fig. 3a and Fig. S3a and c). On average, the TH and DY terms tend to reinforce each other, both contributing to a wettening tendency.

In contrast, the overall weaker wettening in future rcp8.5 projections results from a compensation between the DY term and the TH term (where the latter moistens monsoons as the climate warms) (Fig. 3b and Fig. S4). The substantial drying of the North American monsoon arises mainly from a strong weakening of the mean circulation (DY term, Table 1). On the other hand, the TH and the DY components feature strong spa-

tial variations in the Indian monsoon region: the TH plays a major role in the wettening tendency over the eastern Indian peninsula, and is responsible for the strong drying on its western part (Fig. S4). However, averaging over the entire domain, the TH term dominates over the DY term, and drives an overall wettening.

These analyses suggest therefore that the wettening and northward shift of NH monsoons in mid-Holocene arises mainly from the strengthening of the mean circulation. On the other hand, the weak monsoon response to anthropogenic forcing in rcp8.5 relative to mid-Holocene is mainly due to a compensation between the thermodynamically driven wettening and a dynamically driven drying, as already pointed out by some previous studies (Seager et al., 2010, 2014; Endo & Kitoh, 2014).

Tropical circulation weakening with warming (i.e. weakening of the DY component in all considered monsoons) is a consequence of increased stability in the tropics where temperature lapse rates follow moist adiabats (Held & Soden, 2006). Over tropical and subtropical continents, the stability increase is not compensated by increases in low-level MSE which reduces convection and moisture convergence from oceans, with an associated reduction in land monsoonal rainfall (Fasullo, 2012). The projected monsoonal circulation weakening relative to mid-Holocene hence represents a constraint for monsoonal rainfall: precipitation squeezes around the tropical ocean in rcp8.5 as the static stability increases, the circulation weakens and continental moisture convergence decreases. Unlike what is seen in rcp8.5, the strengthening of the circulation in mid-Holocene allows for increased moisture convergence over land monsoon regions, with a shift of the tropical precipitation from ocean to land and stronger monsoonal rainfall than projected in rcp8.5.

To further understand, at least qualitatively, the different response of land-ocean monsoonal rainfall in the two climates, we analyze changes in NEI in mid-Holocene and rcp8.5 relative to piControl (Fig. 3 and 4). In mid-Holocene, the NEI response is mainly positive over NH continents relative to piControl primarily because of precession-induced insolation changes (Fig. 4a). On the other hand, patterns of anomalous NEI are of opposite sign in rcp8.5, with positive values over the tropical ocean. Hence, to compensate for these NEI changes, the mid-Holocene atmospheric circulation needs to export more energy away from land regions, through a strengthening of the associated DY term (Fig. 3). In rcp8.5, increased stability and the absence of such energetic forcing over NH lands,

where the energy budget is controlled by the top of the atmosphere radiation due to the small thermal inertia of land (Neelin & Held, 1987), cause a weakening of the monsoonal circulation an overall decrease of tropical land rainfall relative to mid-Holocene. Fig. 3 shows in fact a systematic NEI increase of  $\sim 8 \text{ W/m}^2$  in mid-Holocene, compared to a weak change ( $< 1 \text{ W/m}^2$ ) in rcp8.5.

## 4 Discussion and Conclusions

Here, we have investigated mechanisms of monsoon moistening and expansion in two climates, mid-Holocene and future climate scenario rcp8.5. In both climates, the simulated NH summer monsoon rainfall is stronger and monsoon area wider than in the pre-industrial era. However, the projected monsoon response to global warming is weaker than in the simulated past, despite a much larger global warming in the former than in the latter.

In rcp8.5, the NH land monsoon is expected to become wetter relative to pre-industrial conditions because the atmospheric specific humidity increase leads to enhanced precipitation (thermodynamic effect). Additionally, the Hadley circulation is projected to expand and weaken in the future (Frierson et al., 2007; Lu et al., 2007; Seidel et al., 2008; D’Agostino et al., 2017) following the widening and the slowdown already observed in recent decades (Hu & Fu, 2007; Birner, 2010; Davis & Rosenlof, 2012; Nguyen et al., 2013; D’Agostino & Lionello, 2017). This weakens the dynamic term of the moisture budget. Therefore, the weak monsoonal rainfall response with global warming generally results from a compensation between the thermodynamic and dynamic terms. The degree of compensation differs strongly among monsoon regions. For instance, in the Indian monsoon the TH component overwhelms the DY component, giving rise to an overall wettening; in the North American monsoon, the DY component is dominant and responsible for a significant drying.

Unlike what happens under greenhouse gas-induced warming, the strengthening of the mean atmospheric flow is the dominant mechanism behind the wettening and widening of NH monsoons in mid-Holocene. The circulation brings more rainfall over land than over ocean, expanding the total NH land-monsoon area further northward than in rcp8.5. In fact, the dynamic response reinforces the thermodynamically driven wettening in mid-Holocene; in contrast the two components partially cancel each other in rcp8.5.

Advances in our theoretical understanding of monsoons allows us to link dynamically-induced precipitation changes to changes in NEI (Chou et al., 2001; Neelin et al., 2003; Byrne & Schneider, 2016). In this framework, monsoonal circulations, as part of the global tropical overturning, export MSE away from their ascending branches. In steady state, the net MSE flux divergence balances the NEI. Therefore to the extent that energy stratification does not change significantly, changes in NEI need to be compensated for by changes in circulation strength. Hence, the different monsoon responses in the two climates can ultimately be related to changes in the forcing itself, which influences differently the NEI over land and over ocean. In fact, the shortwave forcing, which dominates the mid-Holocene, exhibits a stronger land-ocean contrast than the longwave perturbation associated with greenhouse gas increases in rcp8.5 (Fig. S5). In mid-Holocene, the stronger cross-equatorial atmospheric circulation and the enhanced dynamic term are a result of increased energetic input over the continents: the atmospheric circulation must be stronger in order to export energy away from these regions in the past climate. The absence of such energetic forcing over NH lands in rcp8.5 relative to mid-Holocene results in a relative weakening of mean circulation and hence of the associated precipitation. The strengthening of the dynamic component, therefore, represents a key ingredient for monsoon widening and wettening in mid-Holocene. The weakening of the tropical circulation with global warming limits the projected expansion and intensification of the monsoon systems. The degree of compensation between the thermodynamic and dynamic responses with warming remains highly uncertain and might contribute significantly to the inter-model spread in CMIP5 simulations (Stocker et al., 2014).

This process-oriented study takes an important step towards improving our understanding of monsoon dynamics, quantifying the important role of atmospheric circulation changes in monsoonal precipitation changes by comparing and contrasting past and future climates. Our results highlight that mean surface warming and inter-hemispheric contrast in surface warming are poor indicators of the monsoonal precipitation response. Rather, the monsoon response is constrained by the integrated energy balance, which accounts for changes at the surface as well as at the top of the atmosphere. This explains why the mid-Holocene does not represent an analogue for future warming.

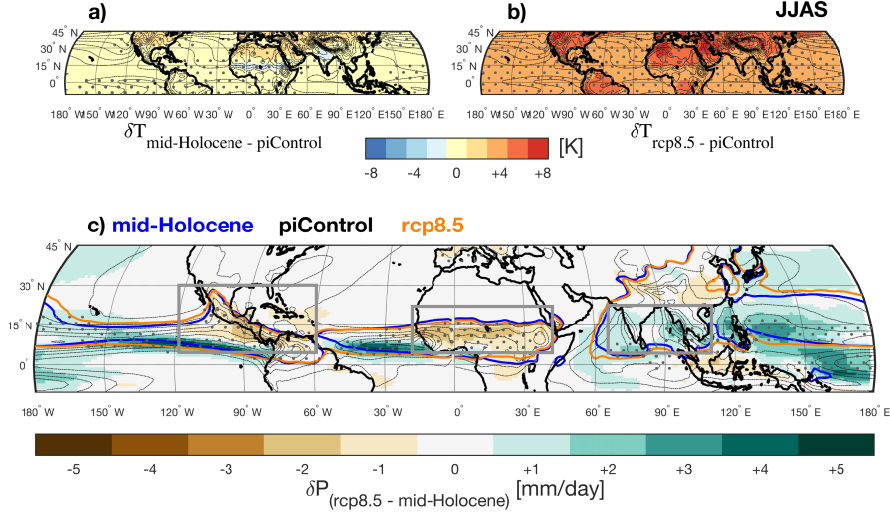


**Figure 1.** Surface temperature difference between mid-Holocene (a) and rcp8.5 (b) and piControl in June-to-September (JJAS) ensemble means (shading). Precipitation difference between rcp8.5 and mid-Holocene JJAS ensemble means (c, shading). Black dashed lines in every panel show the piControl as reference (contour interval 2 K for temperature and 2 mm/day for precipitation). Orange and blue bold lines in c) show areas within which the annual precipitation range (JJAS minus DJFM) exceeds 2 mm/day for rcp8.5 and mid-Holocene, respectively. Grey boxes indicate the North American, African and Indian monsoon domains. Stippling indicates areas where at least 8 out of 9 models agree on the sign of the change.

## Acknowledgments

This study was supported by the JPI - Belmont Forum's project PaCMEDy - Paleo Constraint on Monsoon Evolution and Dynamics. R.D. conceived and designed the study, analyzed the simulations and prepared the manuscript. All authors contributed to the interpretation of the results and the writing of the manuscript. We thank F.S.R. Pausata and Thomas Raddatz for their advice and comments on the draft. We want to acknowledge Nora Specht for her advice on transient eddy computation for the IPSL model. We acknowledge the World Climate Research Programme's Working Group on Coupled Modelling, which is responsible for CMIP. PMIP3 and CMIP5 data are available at <https://esgf-data.dkrz.de/search/cmip5-dkrz/>. Scripts used in the analysis and other supporting information useful to reproduce the author's work are archived by the Max Planck Institute for Meteorology and can be obtained contacting: [publications@mpimet.mpg.de](mailto:publications@mpimet.mpg.de).

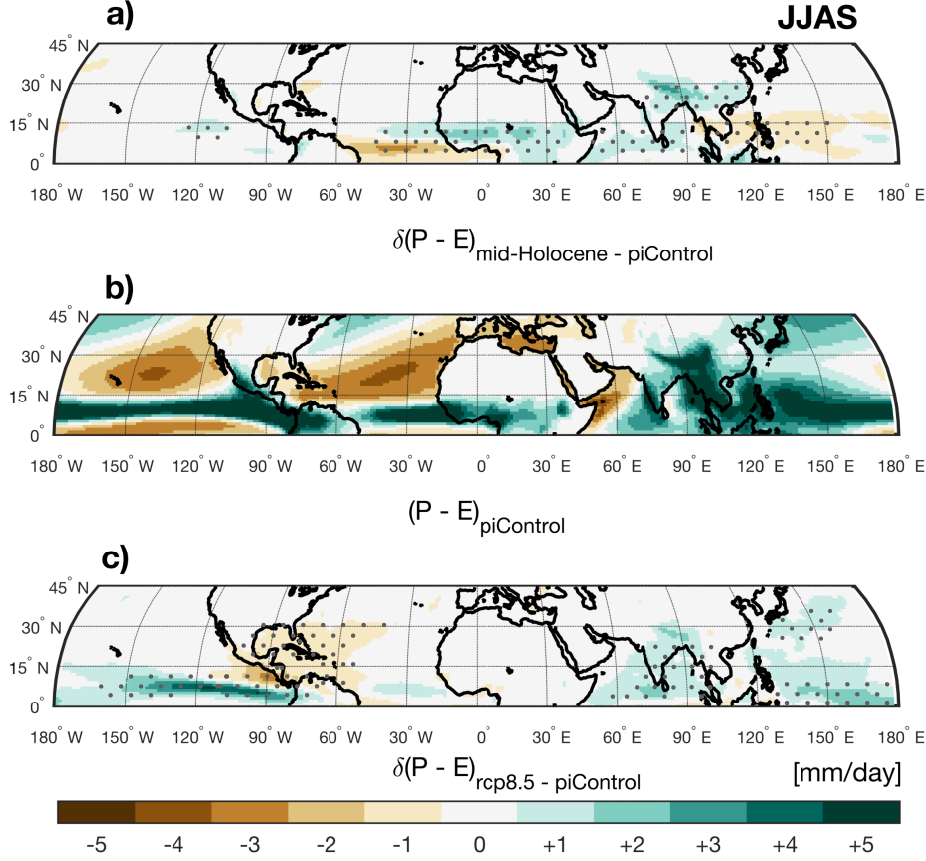


**Figure 2.** Net precipitation difference between the mid-Holocene (a) and the rcp8.5 (c) relative to *piControl* in June-to-September (JJAS) ensemble means (shading). *PiControl* is also shown as reference (b). Black dashed lines in each panel show the *piControl* as reference (contour interval 20 W/m<sup>2</sup>). Stippling indicates areas where at least where 8 out of 9 models agree on the sign of the change.

## References

- Acosta Navarro, J. C., Ekman, A. M., Pausata, F. S., Lewinschal, A., Varma, V., Seland, Ø., ... Riipinen, I. (2017). Future response of temperature and precipitation to reduced aerosol emissions as compared with increased greenhouse gas concentrations. *Journal of Climate*, 30(3), 939–954.
- Biasutti, M. (2013). Forced Sahel rainfall trends in the CMIP5 archive. *Journal of Geophysical Research: Atmospheres*, 118(4), 1613–1623.
- Biasutti, M., Voigt, A., Boos, W. R., Braconnot, P., Hargreaves, J. C., Harrison, S. P., ... Schumacher, C. (2018). Global energetics and local physics as drivers

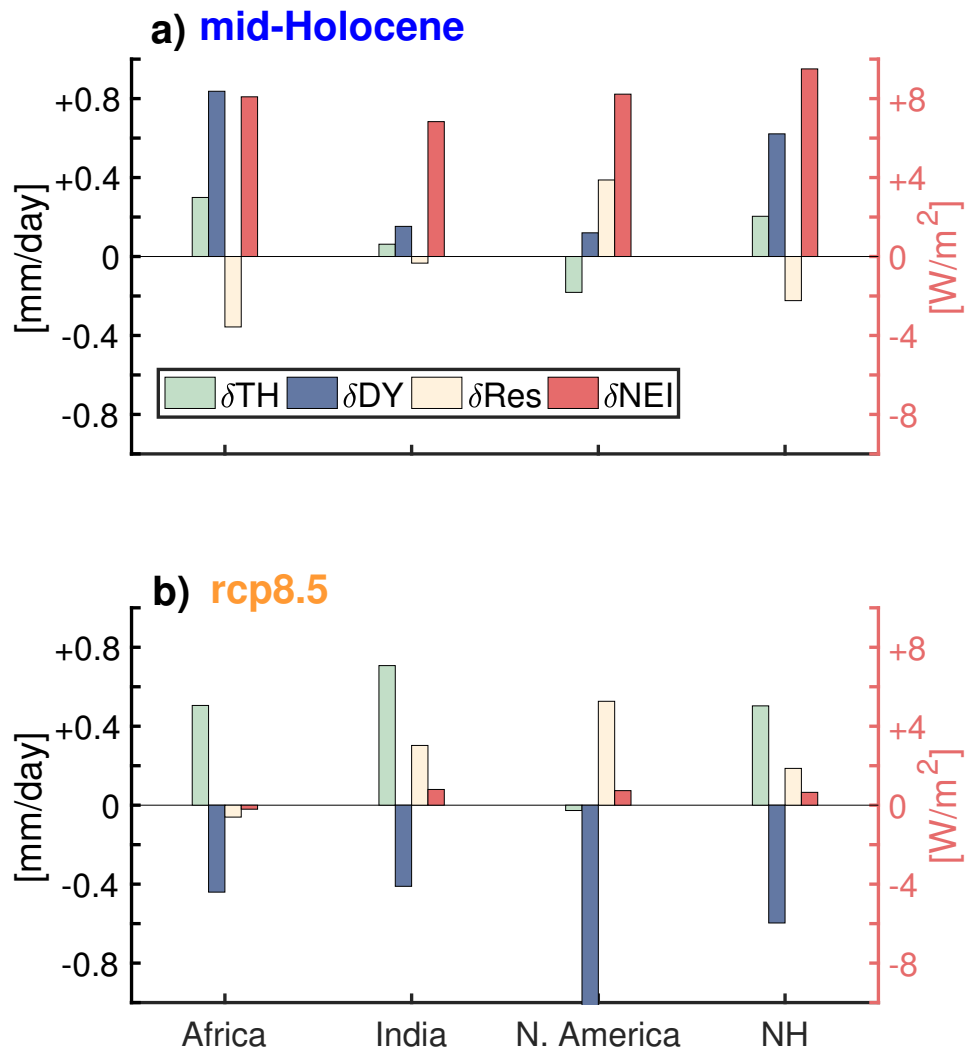


**Figure 3.** Regionally averaged Net Energy Input (NEI - red axis) changes and changes in thermodynamic ( $\delta TH$ ) and dynamic ( $\delta DY$ ) components of the moisture budget, as well as its residual ( $\delta Res$ ) (see Eq.1) for mid-Holocene (a) and rcp8.5 (b) (black axis). Note that 8 out of 9 models agree on the sign of the change.

of past, present and future monsoons. *Nature Geoscience*, 11(6), 392.

Birner, T. (2010). Recent widening of the tropical belt from global tropopause statistics: Sensitivities. *J. Geophys. Res.*, 115, D23109. doi: 10.1029/2010JD014664

Bischoff, T., Schneider, T., & Meckler, A. N. (2017). A conceptual model for the response of tropical rainfall to orbital variations. *Journal of Climate*, 30(20), 8375–8391.



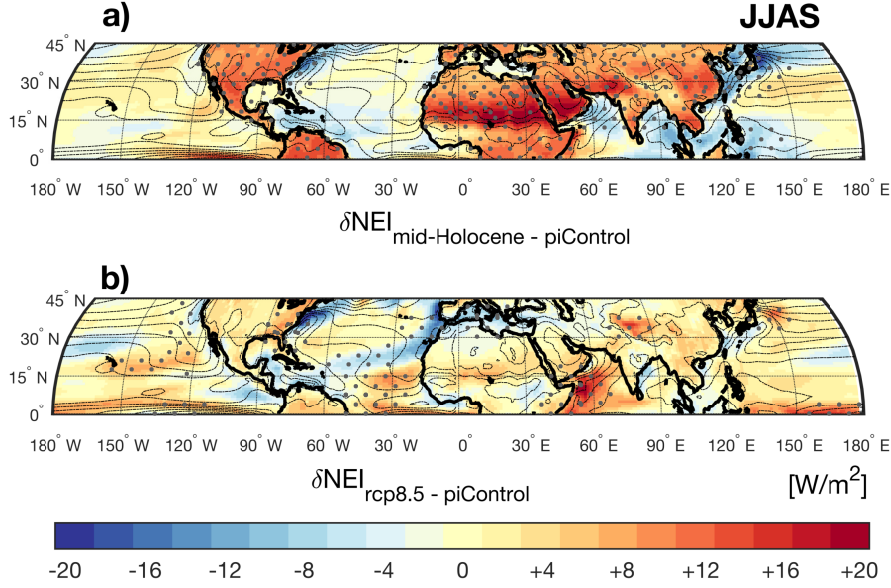


**Figure 4.** Net energy input (NEI) difference between mid-Holocene (a) and rcp8.5 (b) relative to piControl in June-to-September (JJAS) ensemble means (shading). Stippling indicates areas where at least 8 out of 9 models agree on the sign of the change.

**Table 1.** Changes in mid-Holocene and rcp8.5 land monsoon extent and strength relative to piControl. Standard errors for piControl models are reported in brackets. The monsoon extent is calculated inside each monsoon domain where the difference between JJAS and DJFM precipitation exceeds 2 mm/day, as shown in solid lines in Fig. 1.

Monsoons	Extent (10° Km)			Strength (mm/day)			ITCZ (lat. degs)			$\phi Pr > 2\text{mm/day}$		
	piControl	mid-Holocene	rcp8.5	piControl	mid-Holocene	rcp8.5	piControl	mid-Holocene	rcp8.5	piControl	mid-Holocene	rcp8.5
African	5.2 ( $\pm 0.7$ )	+15.4%	+4.4%	5.3 ( $\pm 11.0$ )	+20.3%	+1.2%	7.5	8.4	7.5	14.2	15.4	14.2
Indian	3.1 ( $\pm 0.4$ )	+9.2%	+7.4%	8.5 ( $\pm 1.3$ )	+1.6%	+4.8%	11.5	11.6	11.4	21.8	22.9	22.6
North American	2.8 ( $\pm 0.5$ )	+3.7%	-4.3%	5.8 ( $\pm 1.3$ )	+7.8%	-5.8%	8.1	8.3	7.7	20.1	20.0	21.6
NH	9.3 ( $\pm 1.0$ )	+15.1%	+4.8%	7.0 ( $\pm 0.5$ )	+1.1%	-1.8%	7.9	7.9	7.2	19.2	19.6	18.2

Boos, W. R., & Korty, R. L. (2016). Regional energy budget control of the intertropical convergence zone and application to mid-Holocene rainfall. *Nature Geoscience*, 9(12), 892.

Bordoni, S., & Schneider, T. (2008). Monsoons as eddy-mediated regime transitions of the tropical overturning circulation. *Nature Geoscience*, 1(8), 515.

Braconnot, P., Harrison, S. P., Kageyama, M., Bartlein, P. J., Masson-Delmotte, V., Abe-Ouchi, A., ... Zhao, Y. (2012). Evaluation of climate models using palaeoclimatic data. *Nature Climate Change*, 2(6), 417–424.

- 386 Braconnot, P., Joussaume, S., Marti, O., & De Noblet, N. (1999). Synergistic  
387 feedbacks from ocean and vegetation on the African monsoon response to  
388 mid-Holocene insolation. *Geophysical Research Letters*, 26(16), 2481–2484.
- 389 Broström, A., Coe, M., Harrison, S., Gallimore, R., Kutzbach, J., Foley, J., ...  
390 Behling, P. (1998). Land surface feedbacks and palaeomonsoons in Northern  
391 Africa. *Geophysical Research Letters*, 25(19), 3615–3618.
- 392 Byrne, M. P., & Schneider, T. (2016). Narrowing of the ITCZ in a warming climate:  
393 Physical mechanisms. *Geophysical Research Letters*, 43(21).
- 394 Chen, J., & Bordoni, S. (2014). Orographic effects of the Tibetan Plateau on the  
395 East Asian summer monsoon: An energetic perspective. *Journal of Climate*,  
396 27(8), 3052–3072.
- 397 Chou, C., Neelin, J., & Su, H. (2001). Ocean-atmosphere-land feedbacks in an  
398 idealized monsoon. *Quarterly Journal of the Royal Meteorological Society*,  
399 127(576), 1869–1891.
- 400 Claussen, M., Bathiany, S., Brovkin, V., & Kleinen, T. (2013). Simulated climate–  
401 vegetation interaction in semi-arid regions affected by plant diversity. *Nature*  
402 *Geoscience*, 6(11), 954.
- 403 Claussen, M., & Gayler, V. (1997). The greening of the Sahara during the mid-  
404 Holocene: results of an interactive atmosphere-biome model. *Global Ecology*  
405 *and Biogeography Letters*, 369–377.
- 406 Compo, G. P., & Sardeshmukh, P. D. (2009). Oceanic influences on recent continen-  
407 tal warming. *Climate Dynamics*, 32(2-3), 333–342.
- 408 Cook, B., & Seager, R. (2013). The response of the North American Monsoon to in-  
409 creased greenhouse gas forcing. *Journal of Geophysical Research: Atmospheres*,  
410 118(4), 1690–1699.
- 411 D’Agostino, R., Lionello, P., Adam, O., & Schneider, T. (2017). Factors controlling  
412 Hadley circulation changes from the Last Glacial Maximum to the end of the  
413 21st century. *Geophysical Research Letters*, 44(16), 8585–8591.
- 414 Davis, S. M., & Rosenlof, K. H. (2012). A multidiagnostic intercomparison of  
415 tropical-width time series using reanalyses and satellite observations. *Journal*  
416 *of Climate*, 25(4), 1061–1078.
- 417 Dwyer, J. G., Biasutti, M., & Sobel, A. H. (2012). Projected changes in the seasonal  
418 cycle of surface temperature. *Journal of Climate*, 25(18), 6359–6374.

- 419 D’Agostino, R., & Lionello, P. (2017). Evidence of global warming impact on the  
 420 evolution of the Hadley Circulation in ECMWF centennial reanalyses. *Climate*  
 421 *Dynamics*, 48(9-10), 3047–3060.
- 422 Egerer, S., Claussen, M., & Reick, C. H. (2018). Rapid increase in simulated North  
 423 Atlantic dust deposition due to fast change of Northwest African landscape  
 424 during Holocene. *Climate of the Past*, 14, 1051–1066.
- 425 Endo, H., & Kitoh, A. (2014). Thermodynamic and dynamic effects on regional  
 426 monsoon rainfall changes in a warmer climate. *Geophysical Research Letters*,  
 427 41(5), 1704–1711.
- 428 Fasullo, J. (2012). A mechanism for land–ocean contrasts in global monsoon trends  
 429 in a warming climate. *Climate dynamics*, 39(5), 1137–1147.
- 430 Fasullo, J., & Webster, P. (2003). A hydrological definition of Indian monsoon onset  
 431 and withdrawal. *Journal of Climate*, 16(19), 3200–3211.
- 432 Fleitmann, D., Burns, S. J., Mudelsee, M., Neff, U., Kramers, J., Mangini, A., &  
 433 Matter, A. (2003). Holocene forcing of the Indian monsoon recorded in a  
 434 stalagmite from southern Oman. *Science*, 300(5626), 1737–1739.
- 435 Frierson, D. M., Lu, J., & Chen, G. (2007). Width of the Hadley cell in simple  
 436 and comprehensive general circulation models. *Geophysical Research Letters*,  
 437 34(18).
- 438 Gadgil, S. (2018). The monsoon system: Land–sea breeze or the ITCZ? *Journal of*  
 439 *Earth System Science*, 127(1), 5.
- 440 Gaetani, M., Flamant, C., Bastin, S., Janicot, S., Lavaysse, C., Hourdin, F., ...  
 441 Bony, S. (2017). West African monsoon dynamics and precipitation: The com-  
 442 petition between global SST warming and CO2 increase in CMIP5 idealized  
 443 simulations. *Climate Dynamics*, 48(3-4), 1353–1373.
- 444 Harrison, S. P., Bartlein, P., Izumi, K., Li, G., Annan, J., Hargreaves, J., ...  
 445 Kageyama, M. (2015). Evaluation of CMIP5 palaeo-simulations to improve  
 446 climate projections. *Nature Climate Change*, 5(8), 735.
- 447 Haug, G. H., Hughen, K. A., Sigman, D. M., Peterson, L. C., & Röhl, U. (2001).  
 448 Southward migration of the intertropical convergence zone through the  
 449 Holocene. *Science*, 293(5533), 1304–1308.
- 450 Heaviside, C., & Czaja, A. (2013). Deconstructing the Hadley cell heat transport.  
 451 *Quarterly Journal of the Royal Meteorological Society*, 139(677), 2181–2189.

- 452 Held, I. M., & Soden, B. J. (2006). Robust responses of the hydrological cycle to  
453 global warming. *Journal of Climate*, 19(21), 5686–5699.
- 454 Hély, C., & Lézine, A.-M. (2014). Holocene changes in African vegetation: Tradeoff  
455 between climate and water availability. *Climate of the Past*, 10(2), 681–686.
- 456 Hill, S. A., Ming, Y., & Held, I. M. (2015). Mechanisms of forced tropical meridional  
457 energy flux change. *Journal of Climate*, 28(5), 1725–1742.
- 458 Hsu, P.-c., Li, T., Luo, J.-J., Murakami, H., Kitoh, A., & Zhao, M. (2012). Increase  
459 of global monsoon area and precipitation under global warming: A robust  
460 signal? *Geophysical Research Letters*, 39(6).
- 461 Hsu, P.-c., Li, T., Murakami, H., & Kitoh, A. (2013). Future change of the global  
462 monsoon revealed from 19 CMIP5 models. *Journal of Geophysical Research:  
463 Atmospheres*, 118(3), 1247–1260.
- 464 Hu, Y., & Fu, Q. (2007). Observed poleward expansion of the Hadley circulation  
465 since 1979. *Atmospheric Chemistry and Physics*, 7(19), 5229–5236.
- 466 Jones, G. S., Stott, P. A., & Christidis, N. (2013). Attribution of observed historical  
467 near-surface temperature variations to anthropogenic and natural causes using  
468 CMIP5 simulations. *Journal of Geophysical Research: Atmospheres*, 118(10),  
469 4001–4024.
- 470 Kitoh, A., Endo, H., Krishna Kumar, K., Cavalcanti, I. F., Goswami, P., & Zhou,  
471 T. (2013). Monsoons in a changing world: A regional perspective in a global  
472 context. *Journal of Geophysical Research: Atmospheres*, 118(8), 3053–3065.
- 473 Kutzbach, J., Bonan, G., Foley, J., & Harrison, S. (1996). Vegetation and soil feed-  
474 backs on the response of the African monsoon to orbital forcing in the early to  
475 middle Holocene. *Nature*, 384(6610), 623.
- 476 Lee, J.-Y., & Wang, B. (2014). Future change of global monsoon in the CMIP5. *Cli-  
477 mate Dynamics*, 42(1-2), 101–119.
- 478 Lézine, A.-M., Hély, C., Grenier, C., Braconnot, P., & Krinner, G. (2011). Sahara  
479 and Sahel vulnerability to climate changes, lessons from Holocene hydrological  
480 data. *Quaternary Science Reviews*, 30(21-22), 3001–3012.
- 481 Liu, J., Wang, B., Ding, Q., Kuang, X., Soon, W., & Zorita, E. (2009). Centennial  
482 variations of the global monsoon precipitation in the last millennium: Results  
483 from ECHO-G model. *Journal of Climate*, 22(9), 2356–2371.
- 484 Liu, Z., & Ding, Z. (1998). Chinese loess and the paleomonsoon. *Annual review of*

- 485 *earth and planetary sciences*, 26(1), 111–145.
- 486 Liu, Z., Wang, Y., Gallimore, R., Gasse, F., Johnson, T., Adkins, J., ... Jacob, R.  
 487 (2007). Simulating the transient evolution and abrupt change of Northern  
 488 Africa atmosphere–ocean–terrestrial ecosystem in the Holocene. *Quaternary*  
 489 *Science Reviews*, 26(13-14), 1818–1837.
- 490 Lu, J., Vecchi, G., & Reichler, T. (2007). Expansion of the hadley cell under global  
 491 warming. *Geophysical Research Letters*, 34(6).
- 492 Lu, Z., Miller, P., Zhang, Q., Li, Q., Wårlind, D., Nieradzick, L., ... Smith, B.  
 493 (2018). Dynamic vegetation simulations of the mid-Holocene Green Sahara.  
 494 *Geophysical Research Letters*.
- 495 Merlis, T., Schneider, T., Bordoni, S., & Eisenman, I. (2013). Hadley circulation  
 496 response to orbital precession. Part I: Aquaplanets. *Journal of Climate*, 26(3),  
 497 740–753.
- 498 Neelin, J., Chou, C., & Su, H. (2003). Tropical drought regions in global warming  
 499 and El-niño teleconnections. *Geophysical Research Letters*, 30(24).
- 500 Neelin, J., & Held, I. (1987). Modeling tropical convergence based on the moist  
 501 static energy budget. *Monthly Weather Review*, 115(1), 3–12.
- 502 Nguyen, H., Evans, A., Lucas, C., Smith, I., & Timbal, B. (2013). The Hadley  
 503 Circulation in reanalyses: Climatology, variability, and change. *Journal of Cli-*  
 504 *mate*, 26(10).
- 505 Pascale, S., Boos, W. R., Bordoni, S., Delworth, T., Kapnick, S., Murakami, H., ...  
 506 Zhang, W. (2017). Weakening of the North American monsoon with global  
 507 warming. *Nature Climate Change*, 7(11), 806.
- 508 Pausata, F., Messori, G., & Zhang, Q. (2016). Impacts of dust reduction on the  
 509 northward expansion of the African monsoon during the Green Sahara period.  
 510 *Earth and Planetary Science Letters*, 434, 298–307.
- 511 Schneider, T., Bischoff, T., & Haug, G. H. (2014). Migrations and dynamics of the  
 512 intertropical convergence zone. *Nature*, 513(7516), 45–53.
- 513 Schulz, H., von Rad, U., & Erlenkeuser, H. (1998). Correlation between Arabian  
 514 Sea and Greenland climate oscillations of the past 110,000 years. *Nature*,  
 515 393(6680), 54.
- 516 Seager, R., Liu, H., Henderson, N., Simpson, I., Kelley, C., Shaw, T., ... Ting,  
 517 M. (2014). Causes of increasing aridification of the Mediterranean region in

- 518 response to rising greenhouse gases. *Journal of Climate*, 27(12), 4655–4676.
- 519 Seager, R., Naik, N., & Vecchi, G. A. (2010). Thermodynamic and dynamic mech-  
 520 anisms for large-scale changes in the hydrological cycle in response to global  
 521 warming. *Journal of Climate*, 23(17), 4651–4668.
- 522 Seidel, D. J., Fu, Q., Randel, W. J., & Reichler, T. J. (2008). Widening of the tropi-  
 523 cal belt in a changing climate. *Nature geoscience*, 1(1), 21–24.
- 524 Seth, A., Rauscher, S. A., Biasutti, M., Giannini, A., Camargo, S. J., & Rojas, M.  
 525 (2013). CMIP5 projected changes in the annual cycle of precipitation in mon-  
 526 soon regions. *Journal of Climate*, 26(19), 7328–7351.
- 527 Seth, A., Rauscher, S. A., Rojas, M., Giannini, A., & Camargo, S. J. (2011). En-  
 528 hanced spring convective barrier for monsoons in a warmer world? *Climatic*  
 529 *Change*, 104(2), 403–414.
- 530 Seth, A., Rojas, M., & Rauscher, S. A. (2010). CMIP3 projected changes in the  
 531 annual cycle of the South American monsoon. *Climatic Change*, 98(3-4), 331–  
 532 357.
- 533 Stocker, T. F., Qin, D., Plattner, G.-K., Tignor, M., Allen, S. K., Boschung, J., ...  
 534 Midgley, P. M. (2014). *Climate change 2013: The physical science basis*.  
 535 Cambridge University Press Cambridge, UK, and New York.
- 536 Sutton, R. T., Dong, B., & Gregory, J. M. (2007). Land/sea warming ratio in  
 537 response to climate change: IPCC AR4 model results and comparison with  
 538 observations. *Geophysical Research Letters*, 34(2).
- 539 Swann, A. L., Fung, I. Y., Liu, Y., & Chiang, J. C. (2014). Remote vegetation feed-  
 540 backs and the mid-Holocene Green Sahara. *Journal of Climate*, 27(13), 4857–  
 541 4870.
- 542 Tanaka, H., Ishizaki, N., & Nohara, D. (2005). Intercomparison of the intensities  
 543 and trends of Hadley, Walker and monsoon circulations in the global warming  
 544 projections. *SOLA*, 1, 77–80.
- 545 Tierney, J. E., & Pausata, F. S. (2017). Rainfall regimes of the Green Sahara. *Sci-*  
 546 *ence advances*, 3(1), e1601503.
- 547 Tjallingii, R., Claussen, M., Stuut, J.-B. W., Fohlmeister, J., Jahn, A., Bickert, T.,  
 548 ... Röhl, U. (2008). Coherent high-and low-latitude control of the northwest  
 549 African hydrological balance. *Nature Geoscience*, 1(10), 670.
- 550 Trenberth, K. E., & Guillemot, C. J. (1995). Evaluation of the global atmospheric

- 551 moisture budget as seen from analyses. *Journal of Climate*, 8(9), 2255–2272.
- 552 Trenberth, K. E., Stepaniak, D. P., & Caron, J. M. (2000). The global monsoon  
553 as seen through the divergent atmospheric circulation. *Journal of Climate*,  
554 13(22), 3969–3993.
- 555 Vamborg, F., Brovkin, V., & Claussen, M. (2010). The effect of a dynamic back-  
556 ground albedo scheme on Sahel/Sahara precipitation during the mid-holocene.  
557 *Climate of the Past Discussions*, 6, 2335–2370.
- 558 Vecchi, G. A., & Soden, B. J. (2007). Global warming and the weakening of the  
559 tropical circulation. *Journal of Climate*, 20(17), 4316–4340.
- 560 Walker, J. (2017). *Seasonal and interannual variability in South Asian monsoon*  
561 *dynamics* (Unpublished doctoral dissertation). California Institute of Technol-  
562 ogy.
- 563 Wang, Y., Cheng, H., Edwards, R. L., Kong, X., Shao, X., Chen, S., . . . An, Z.  
564 (2008). Millennial and orbital-scale changes in the East Asian monsoon over  
565 the past 224,000 years. *Nature*, 451(7182), 1090.
- 566 Webster, P., & Fasullo, J. (2002). Monsoon— dynamical theory. *Encycl. Atmos.*  
567 *Sci.*, 1370–1385.
- 568 Weldeab, S., Lea, D. W., Schneider, R. R., & Andersen, N. (2007). 155,000 years of  
569 west African monsoon and ocean thermal evolution. *science*, 316(5829), 1303–  
570 1307.
- 571 Yuan, D., Cheng, H., Edwards, R. L., Dykoski, C. A., Kelly, M. J., Zhang, M., . . .  
572 Wu, J. (2004). Timing, duration, and transitions of the last interglacial Asian  
573 monsoon. *Science*, 304(5670), 575–578.
- 574 Zhao, Y., Braconnot, P., Marti, O., Harrison, S., Hewitt, C., Kitoh, A., . . . Weber,  
575 S. (2005). A multi-model analysis of the role of the ocean on the African  
576 and Indian monsoon during the mid-Holocene. *Climate Dynamics*, 25(7-8),  
577 777–800.
- 578 Zhao, Y., & Harrison, S. (2012). Mid-Holocene monsoons: A multi-model analysis of  
579 the inter-hemispheric differences in the responses to orbital forcing and ocean  
580 feedbacks. *Climate Dynamics*, 39(6), 1457–1487.
- 581 Zhisheng, A., Guoxiong, W., Jianping, L., Youbin, S., Yimin, L., Weijian, Z., . . .  
582 Jiangyu, M. (2015). Global monsoon dynamics and climate change. *Annual*  
583 *Review of Earth and Planetary Sciences*, 43, 29–77.

584     Zhou, T., Zhang, L., & Li, H. (2008). Changes in global land monsoon area and to-  
585     tal rainfall accumulation over the last half century. *Geophysical Research Let-*  
586     *ters*, 35(16).